Nuclear Medicine of Hepatobiliary System (SPECT and PET)

Pietro Zucchetta and Diego Cecchin

Contents

Abstract

Nuclear medicine techniques allow the functional evaluation of the liver and the biliary system. Biliary scintigraphy using technetiated iminodiacetic acid (IDA) derivatives explores the biliary excretion from the uptake at the vascular pole of the hepatocyte to the bile excretion in the intestinal lumen. Positron Emission Tomography (PET), either in a PET/CT scanner or in a PET/MR tomograph, relies on 18F-fluoro-deoxy-glucose (18F-FDG) or labelled choline to detect more aggressive and less aggressive hepato-cellular carcinomas (HCC) respectively. Neuroendocrine tumors arising in the gastroenteric tract or in the pancreas (NET-GEP) are best evaluated by DOTA compounds (DOTATOC, DOTANOC, and DOTANOE), labelled with 68Ga. They share a high affinity for the SSR-2, which is widely expressed in NET-GEP and represents an excellent opportunity for the evaluation of the primary tumor and the metastatic disease, including the liver.

1 Introduction

The liver is divided into two lobes (right and left lobe) and is characterized by a double blood supply (hepatic artery arising from the celiac trunk and portal vein, draining the GI tract) mixing at the capillary level in the hepatic sinusoids.

Functional liver anatomy is segmental, based on the distribution of arterial, portal, and biliary system (left lobe: S2, S3; right lobe: S4, S5, S6, S7, S8; S1 is functionally independent).

1.1 Biliary Scintigraphy

Biliary scintigraphy allows the evaluation of the hepatocyte function (radiopharmaceutical uptake

P. Zucchetta (✉) · D. Cecchin
Nuclear Medicine Department,
Padua University Hospital, Padua, Italy
e-mail: pietro.zucchetta@unipd.it;
diego.cecchin@unipd.it

E. Quaia (ed.), *Imaging of the Liver and Intra-hepatic Biliary Tract*,
Medical Radiology, Diagnostic Imaging, https://doi.org/10.1007/978-3-030-38983-3_6

at the vascular pole of the hepatocyte) and of the bile excretion.

1.1.1 Radiopharmaceuticals

The radiopharmaceuticals used for the hepatic-biliary scintigraphy are derivatives of the iminodiacetic acid (IDA). They are labelled with ^{99m}Tc and are taken up from the bloodstream, after intravenous injection, from the vascular pole of the hepatocyte, sharing the transporter with endogenous bilirubin. The most frequently used molecules are disofenin (DISIDA) and mebrofenin (bromide) (Figs. 1 and 2).

The excretion at the biliary pole is fast, because these compounds are not conjugated with glucuronic acid, as is the case for bilirubin; therefore they appear in the biliary system in few minutes and their concentration in liver parenchyma is usually halved in 15–20 min after the maximum uptake, usually reached in 3–5 min.

Since endogenous bilirubin competes for the same membrane transporter, hyperbilirubinemia, as in jaundice, can impair the radiopharmaceutical uptake. In this case, the standard dose (around 185 MBq in adults) can be increased proportionally, to guarantee an adequate visualization of the liver and the biliary system.

1.1.2 Patient Preparation

Patients should fast for 6–10 h (minimum 4 h, maximum 24 h). Of note, the fasting period must not exceed 24 h, to avoid excessive bile concentration and retention in the biliary tree, which can determine false-positive readings. The same consideration applies to total parenteral nutrition. Therefore, it is advisable to postpone the examination or, alternatively, to pretreat the patient with cholecystokinetic drugs (e.g., sincalide), if allowed.

Smoking and alcohol consumption should be avoided during the 24 h preceding the examination, because they can interfere with radiopharmaceutical absorption and/or excretion.

Some drugs may influence the sphincter of Oddi function (e.g., opiates) or gallbladder contraction (atropine, somatostatin analogues, sincalide). It is possible to exploit some pharmacological effects to test, for instance, the gallbladder filling, administering morphine, or gallbladder contraction after sincalide.

Therefore, a detailed pharmacological history is mandatory during the examination, as in most scintigraphic studies.

When biliary atresia is suspected in neonates and infants, it is highly recommended to prevent abdominal skin contamination due to micturition. The positioning of a urine-collection bag will markedly simplify image interpretation.

1.1.3 Acquisition Protocol

Dynamic acquisition (matrix 128 × 128, 30–60 s/frame) in the anterior projection (patient lying supine) starts immediately after i.v. tracer injection, using a large field-of-view (LFOV) gamma camera, fitted with a low-energy high-resolution (LEHR) parallel-hole collimator.

The field of view includes the whole liver, the upper abdomen, and at least a portion of the cardiac region.

The usual duration of the acquisition is between 45 and 60 min. Delayed images are acquired (most often after a lipid-rich meal) as the clinical situation requires (e.g., non-visualization of the bowel), up to 24 h after injection.

Tomographic images (single-photon emission tomography, SPET) can be useful when a biliary leakage is suspected, particularly if hybrid SPET/CT is available.

A double-head gamma camera is preferred, fitted with LEHR parallel-hole collimator, to keep the acquisition duration around 25–30 min (matrix 128 × 128, 360 degrees orbit, 120 frames, 25–30 s/frame).

1.1.4 Image Evaluation

Visual evaluation of all the images represents the first essential step. The parameters to consider are liver uptake, visualization of the intrahepatic tree and extrahepatic biliary ducts, gallbladder visualization (if any), and timing of radiotracer appearance in the small bowel.

Time-activity curves (region of interest drawn on heart, liver, main branches of the biliary tree and bile ducts, gallbladder, and small bowel) may help in image interpretation. The most used

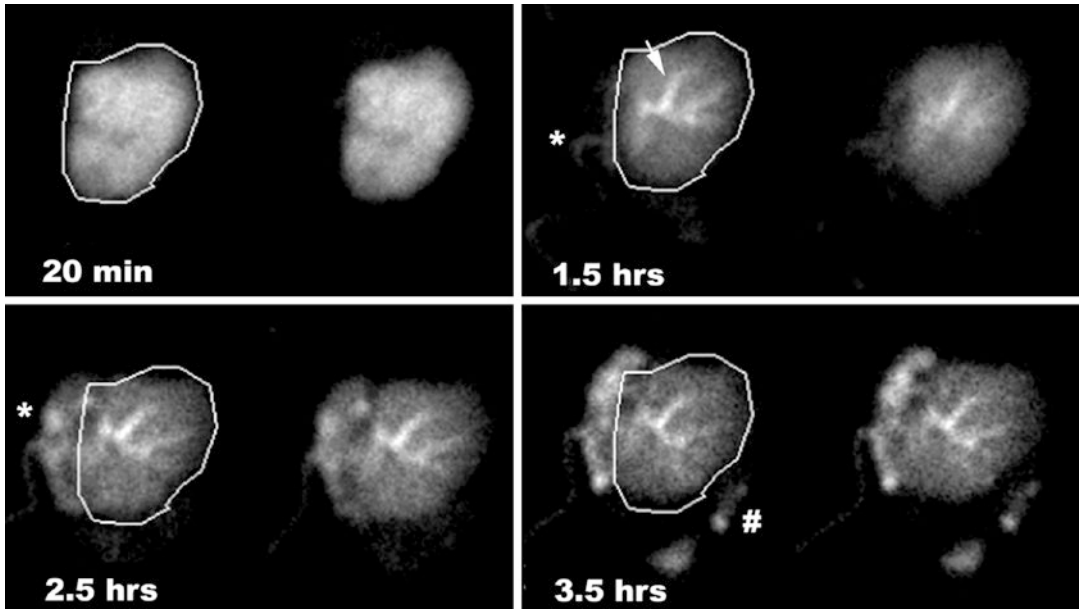

Fig. 1 ^{99m}Tc-IDA derivates in a child after S2–S3 left split liver transplantation. Upper left: two frames (5 min each) 20 min after the injection demonstrating good uptake of the graft. Upper right: two frames (5 min each) 1.5 h after injection showing dilatation of the intrahepatic biliary tree (white arrow) and initial visualization of the drainage (asterisk), clearly visible at 2.5 and 3.5 h. At 3.5 h the biliodigestive anastomosis (hash) can be seen

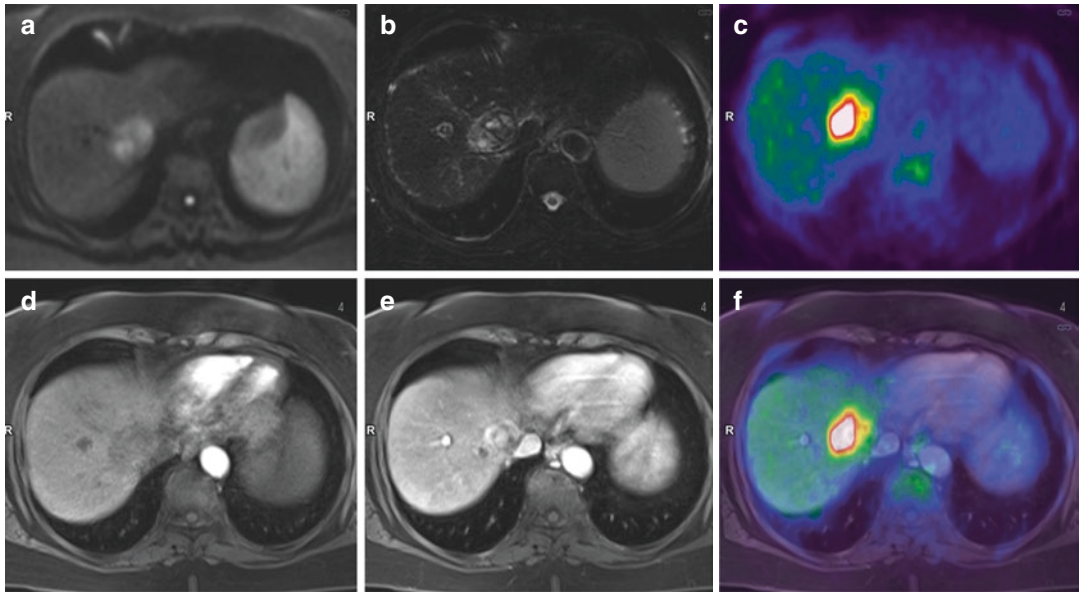

Fig. 2 18F-FDG PET/MR in a patient affected by hepatocellular carcinoma. In S8 an area of intense uptake (SUV Max 11) of the radiopharmaceutical corresponding to the lateral portion of an area (40 × 30 mm) previously treated. (**a**) DWI (b800); (**b**) T2 TSE fat saturated; (**c**) 18F-FDG PET; (**d**) T1 postcontrast (arterial phase); (**e**) T1 postcontrast (venous phase); (**f**): fused **c** + **e**

numerical parameters are liver-Tmax (time needed to reach the maximal activity in liver parenchyma), liver-T50 (time needed to reach 50% of maximum activity), and gallbladder ejection fraction (the percentage difference in background-corrected activity between maximum gallbladder filling and post-emptying image).

Circulating activity decreases fast in normal patients, reaching a nadir in around 5 min. The liver parenchymal uptake shows an early increase, with a maximum between 10 and 20 min postinjection, followed by a fast decrease, leaving very low activity at 60 min.

The intrahepatic biliary tree is usually visualized between 5 and 20 min postinjection, whereas the visualization of the gallbladder is highly variable, depending on its filling status and on the contraction/relaxation of the sphincter of Oddi.

The radiotracer usually reaches the small bowel in 20–40 min.

Bowel non-visualization, even after 24 h, is highly suggestive of biliary atresia in icteric neonates and infants, whereas biliary obstruction leads to variable delays in bile outflow and bowel visualization.

Acute cholecystitis is characterized by non-visualization of the gallbladder, even 60 min postinjection and after morphine administration. Sometimes, a thin rim of enhanced uptake is present in the gallbladder bed (rim sign).

The radiotracer appears in the abdominal cavity in case of biliary leakage.

Bilio-digestive anastomosis, using a bowel loop as biliary reservoir, is prone to acute and chronic cholangitis and the hepatic-biliary scintigraphy can identify the stasis in a malfunctioning bowel loop, which is a major risk factor.

1.1.5 Main Indications

Functional assessment of biliary function/post-surgical hyperplasia

Biliary atresia

Integrity of biliary tree/biliary extravasation

Acute cholecystitis

Patency of bilio-enteric surgical anastomosis

Enterogastric reflux

1.2 Liver PET Studies

Positron-emission tomography (PET) uses positron-emitting radiopharmaceuticals and plays a crucial role in many diagnostic protocols, particularly in oncology, where the most widely used tracer is 18F-fluoro-deoxy-glucose (18F-FDG). PET scans are typical hybrid examinations, obtained on a combined PET and CT scanner (PET/CT). In recent years the first clinical hybrid PET/MR scanners have been introduced, opening exciting perspectives.

18F-FDG depicts the glucose metabolism and shows a physiologic uptake in the liver parenchyma. Therefore, it is useful to identify lesions with metabolic activity greater than the surrounding liver, as in the case of most metastatic lesions and in cholangiocarcinoma.

The glycolytic activity of hepatocellular carcinoma (HCC) does not differ, in many cases, from the normal liver metabolism, but increases significantly in high-grade lesions, when the tumor becomes more aggressive and is less differentiated. Therefore, the degree of 18F-FDG uptake corresponds roughly to the aggressiveness of HCC and can contribute to the grading of the disease.

Labelled choline, either with 11C or with 18F, detects low-grade HCC and has been proposed to stage at least the more complex cases of HCC, particularly aiming at extrahepatic disease.

18F-FDG and labelled choline are ideal candidates for the characterization of doubtful hepatic lesions, as is the case in multifocal disease after treatment, whether by TACE or by microwave ablation. The introduction of hybrid PET/MR scanners opens further perspectives in this evolving field.

Metastatic liver involvement at diagnosis is frequent in neuroendocrine tumors arising in the gastroenteric tract or in the pancreas (NET-GEP). NET-GEP metastasis shows a variable uptake of 18F-FDG, which is proportional to their aggressiveness. The same holds true for the primary tumor, which is often very small. Somatostatin receptors (SSR) are highly expressed in the vast majority of NET-GEP and radiolabelled com-

pounds have been targeted both to their diagnosis and treatment. The most efficient PET radiopharmaceuticals are the DOTA compounds (DOTATOC, DOTANOC, and DOTANOE), labelled with 68Ga. They share a high affinity for the SSR-2, which is widely expressed in NET-GEP and represents an excellent opportunity for the evaluation of the primary tumor and of the metastatic disease, including the liver.

The treatment of metastatic NET-GEP is often difficult, even if they are often slow-growing tumors, because the disease can be already diffuse at the diagnosis. Radiometabolic therapy can control the disease with very limited side effects, using for instance DOTATE labeled with a beta-emitter (177 LU). The integrated approach of lesion characterization and radio-metabolic treatment represents a classical example of theranostics.

Further Reading

Barseghyan K, Ramanathan R, Chavez T, Harlan S, Lin CH, Mitsinikos T, McLean C (2018) Utility of hepatobiliary scintigraphy in diagnosing or excluding biliary atresia in premature neonates and full-term infants with conjugated hyperbilirubinemia who received parenteral nutrition. J Matern Fetal Neonatal Med 31(24):3249–3254

Bodei L, Weber WA (2018) Somatostatin receptor imaging of neuroendocrine tumors: from agonists to antagonists. J Nucl Med 59(6):907–908

Bodei L, Kwekkeboom DJ, Kidd M, Modlin IM, Krenning EP (2016) Radiolabeled somatostatin analogue therapy of gastroenteropancreatic cancer. Semin Nucl Med 46(3):225–238

Bodei L, Ambrosini V, Herrmann K, Modlin I (2017) Current concepts in(68)Ga-DOTATATE imaging of neuroendocrine neoplasms: interpretation, biodistribution, dosimetry, and molecular strategies. J Nucl Med 58(11):1718–1726

Christensen CT, Peacock JG, Vroman PJ, Banks KP (2018) Scintigraphic findings beyond ejection fraction on hepatobiliary scintigraphy: are they correlated with chronic gallbladder disease? Clin Nucl Med 43(10):721

Cremonesi M, Ferrari ME, Bodei L, Chiesa C, Sarnelli A, Garibaldi C, Pacilio M, Strigari L, Summers PE, Orecchia R, Grana CM, Botta F (2018) Correlation of dose with toxicity and tumour response to (90)Y- and (177)Lu-PRRT provides the basis for optimization through individualized treatment planning. Eur J Nucl Med Mol Imaging 45(13):2426–2441

Hepatobiliary (2019). http://snmmi.files.cms-plus.com/docs/Hepatobiliary_Scintigraphy_V4.0b.pdf. Accessed 15 June 2019

Kim JR, Hwang JY, Yoon HM, Jung AY, Lee JS, Kim JS, Namgoong JM, Kim DY, Oh SH, Kim KM, Cho YA (2018) Risk estimation for biliary atresia in patients with neonatal cholestasis: development and validation of a risk score. Radiology 288(1):262–269

Krishnamurthy GT, Krishnamurthy S (2009) Nuclear hepatology: a textbook of hepatobiliary diseases, 2nd edn. Springer, Berlin. ISBN: 978-3-642-00647-0

Liao X, Wei J, Li Y, Zhong J, Liu Z, Liao S, Li Q, Wei C (2018) 18F-FDG PET with or without CT in the diagnosis of extrahepatic metastases or local residual/recurrent hepatocellular carcinoma. Medicine (Baltimore) 97(34):e11970

Mallick B, Bhattacharya A, Gupta P, Rathod S, Dahiya D, Dutta U (2018) Cholecystocolic fistula diagnosis with hepatobiliary scintigraphy: a case report. JGH Open 3(1):91–93. https://doi.org/10.1002/jgh3.12104. eCollection 2019 Feb

Mandelia A, Lal R, Mutt N (2017) Role of hepatobiliary scintigraphy and preoperative liver biopsy for exclusion of biliary atresia in neonatal cholestasis syndrome. Indian J Pediatr 84(9):685–690

Matesan M, Bermo M, Cruite I, Shih CH, Elojeimy S, Behnia F, Lewis D, Vesselle H (2017) Biliary leak in the postsurgical abdomen: a primer to HIDA scan interpretation. Semin Nucl Med 47(6):618–629

Miner LT, Tulchinsky M (2018) Detecting intestinal malrotation on hepatobiliary scintigraphy: making a case for a better standardized reporting template. Clin Nucl Med 43(4):289–293

Oberg K, Krenning E, Sundin A, Bodei L, Kidd M et al (2016) A Delphic consensus assessment: imaging and biomarkers in gastroenteropancreatic neuroendocrine tumor disease management. Endocr Connect 5(5):174–187

Rassam F, Zhang T, Cieslak KP, Lavini C, Stoker J, Bennink RJ, van Gulik TM, van Vliet LJ, Runge JH, Vos FM (2019) Comparison between dynamic gadoxetate-enhanced MRI and (99m)Tc-mebrofenin hepatobiliary scintigraphy with SPECT for quantitative assessment of liver function. Eur Radiol 29:5063

Smit Duijzentkunst DA, Kwekkeboom DJ, Bodei L (2017) Somatostatin receptor 2-targeting compounds. J Nucl Med 58(Suppl 2):54S–60S

Snyder E, Lopez PP (2019) Hepatobiliary Iminodiacetic Acid (HIDA) scan. 2019 mar 25.StatPearls [internet]. StatPearls Publishing, Treasure Island, FL. http://www.ncbi.nlm.nih.gov/books/NBK539781/

Vélez-Gutierrez C, Gutierrez-Villamil C, Arevalo-Leal S, Mejía-Hernandez G, Marín-Oyaga V (2019) Hepatobiliary scintigraphy in the study of complications in adult patients after liver transplant. Description of the experience. Rev Esp Med Nucl Imagen Mol 38(4):207–211

Wang L, Yang Y, Chen Y, Zhan J (2018) Early differential diagnosis methods of biliary atresia: a meta-analysis. Pediatr Surg Int 34(4):363–380. Review

Watanabe A, Harimoto N, Araki K, Yoshizumi T, Arima K, Yamashita Y, Baba H, Tetsuya H, Kuwano H, Shirabe K (2018) A new strategy based on fluorodeoxyglucose-positron emission tomography for managing liver metastasis from colorectal cancer. J Surg Oncol 118(7):1088–1095

Yamamoto M, Tahara H, Hamaoka M, Shimizu S, Kuroda S, Ohira M, Ide K, Kobayashi T, Ohdan H (2018) Utility of hepatobiliary scintigraphy for recurrent reflux cholangitis following choledochojejunostomy: a case report. Int J Surg Case Rep 42:104–108

Zhang W, Fang C, Liu H, Chen Y (2019) FDG PET/CT imaging of hepatocellular carcinoma with bile duct tumor thrombus. Clin Nucl Med 44(2):130–132